Oil & Gas Science and Technology – Rev. IFP Energies nouvelles **75**, 45 (2020)
© Z. Wang et al., published by IFP Energies nouvelles, 2020
https://doi.org/10.2516/ogst/2020041

Available online at:
ogst.ifpenergiesnouvelles.fr

REGULAR ARTICLE OPEN ACCESS

Experimental investigation on precipitation damage during water alternating flue gas injection

Zhouhua Wang, Yuping Zhang* and Haoqi Liao

State Key Laboratory of Oil and Gas Reservoir Geology and Exploitation, Southwest Petroleum University, No. 8 Xindu Avenue, 610500 Chengdu, PR China

Received: 11 January 2020 / Accepted: 26 May 2020

Abstract. Water Alternating Gas (WAG) approach can improve the efficiency of gas flooding. However, the precipitation damage that is induced by the gas injection may be inevitable. The precipitation pressure point test of gas injection, and the WAG parallel double-tube long-core flooding experiment under different injection conditions were systematically performed to obtain the optimum injection parameters. The variations of petrophysical properties were caused by precipitation, and its morphology was also determined by centrifugal capillary force and environmental scanning electron microscope. The precipitation pressure rised with the increase of the amount of gas injection, generally 2.0 MPa ~ 3.0 MPa higher than the bubble point pressure (P_b), and it was confirmed by X-ray energy spectrum and scanning electron microscope that the precipitation was mainly asphaltene. The optimum injection parameters for WAG were Gas–Water Ratio (GWR) of 1:1 and slug size of 0.1 HydroCarbon Pore Volume (HCPV), which benefited the recovery of low-permeability and high-permeability pipe by additional recovery of 28.5% and 17.4% respectively, while WAG process enhanced the total oil recovery by 23.4%. The pore volume and median radius of capillary pressure of all cores were both reduced with more obvious effects on conglomerate. Combined with the results of sediment saturation, it also showed the poorer the physical properties of the cores, the severer the influence of the precipitation. Overall, the WAG could greatly improve the recovery but the influence of precipitation must be considered.

1 Introduction

Gas injection is an important and effective driving method to enhance oil recovery during the reservoir development. Methods for gas injection include continuous injection, Water Alternating Gas (WAG) injection, and cyclic injection. The gas types include N_2, CO_2, CH_4, hydrocarbon-rich gas, etc. [1]. The widespread WAG has been effectively used in practical applications. Due to the low viscosity of the gas, and the large density difference between the injected gas and the crude oil, poor macroscopic sweep efficiency is observed during the gas injection process, which leads to the oil bypassing at certain parts of the reservoir. The displacement front is unstable and an early breakthrough occurred in the reservoir [2]. This situation is especially exacerbated in reservoirs with strong heterogeneity. The displacement front tends to move along the regions with high permeability, resulting in bypassing considerable amount of residual oil in the less permeable regions [3]. The WAG can reduce the adverse mobility ratio between the injected fluid and the crude oil to mitigate the channeling, to improve the macroscopic sweep efficiency and enable the high displacement efficiency during the gas injection [4]. The WAG is also very cost-effective gas injection by significantly reducing the expenses for purchasing gases [2, 5]. The total amount of injected water and gas, injection schedule and well control should be optimized during the WAG to maximize Net Present Value (NPV) [6]. WAG combines the advantages of Water Flooding (WF) and Gas Injection (GI). Kulkarni and Rao compared the displacement efficiencies of WAG and GI by conducting a series of immiscible and miscible core-flooding experiments, and found out that the performance of WAG injection is superior to GI [7]. Normally, the failure of enhanced oil recovery project is attributed to the reservoir heterogeneity [3]. In low-permeability heterogeneous reservoirs, WF has the disadvantages of poor injectivity, low production rate, high Water–Oil Ratio (WOR) and low recovery [8]. In strongly heterogeneous reservoirs, due to the early gas breakthrough and high gas recirculation rate, it is not feasible to only continuously inject single gas stream when the economic efficiency is the main controlling factor. Theoretically, WAG is one of the most cost-effective technologies for delaying gas breakthrough and lowering mobility ratio [9], but it has similar problems or challenges encountered during WF and GI, early gas breakthrough, injected energy loss,

* Corresponding author: zhangyuping9582@163.com

and asphaltene precipitation [10]. The main purpose of this study is to evaluate the effects of asphaltene precipitation on oil displacement during GI. Therefore, WAG, which combines the features of WF and GI but with better sweep and displacement efficiencies, was adopted for applications in heterogeneous reservoir.

No matter what type of gas injection is performed, asphaltene precipitation is an inevitable problem during the process. The solid deposition seriously affects oil recovery and increases the cost of enhanced oil recovery [11]. When the content of asphaltene reaches a certain limit, the wettability of the reservoir rock tends to be altered from oil-wet to water-wet [12–16], which will cause more reservoir blockage and reduction of heavy oil production [12, 17], and become unfavorable for oil production and recovery process [18–22]. Mansoori and Pacheco-Sanchez *et al.* stated that the process of asphaltene precipitation out of the crude oil is irreversible [23, 24]. According to the solubility definition for asphaltene, it is undissolved in light hydrocarbon solvents such as normal alkanes, olefins, etc., but is soluble in light aromatics such as toluene, benzene, and xylene [25–29]. Thus, solvent can be injected to dissolve asphaltene present in the reservoir and reduce asphaltene precipitation tendency [30]. In addition, asphaltene will severely damage pipelines, separators, equipment near wellbore, and other ground facilities. The formation damage occurs with reduction of relative permeability, and even flow of reservoirs and ground facilities will be interrupted, resulting in low productivity or even no flow rate [31–36]. Some issues pertaining to Health, Safety, and Environment (HSE) can also be generated [37, 38]. Undoubtedly, the asphaltene produced in gas injection and its impact on production have brought some major technical challenges to the petroleum industry [39, 40].

So far, CO_2 injection is the most widely used gas injection technique in conventional reservoirs [41]. Researches on asphaltene precipitation in CO_2 injection are also very common. Asphaltene can cause pore blockage, which reduces oil recovery and results in serious operational problems [42]. During the CO_2 injection, the duration of CO_2 interaction with oil increases, CO_2 continuously penetrates into the oil phase, leading to an increase in asphaltene. As the frequency of CO_2 injection increases, the permeability becomes smaller and smaller due to the precipitaton of asphaltene [43]. Higher gas concentration can also result in higher content of asphaltene precipitaton [44–47]. The better the petrophysical properties, the smaller the influence of asphaltene. For example, the severity of asphaltene precipitation and pore blockage decreases significantly with increasing pore size [42], and similarly, the effects of asphaltene on recovery and permeability decrease with increasing original rock permeability [48].

The effects of asphaltene during CO_2 injection have been widely studied, but few studies have investigated the effects of asphaltene during flue gas injection. During the in-situ combustion process, the combustion belt can be maintained by burning and moving in the formation by continuously injecting air. During the combustion, the oxygen in the injected air is consumed, and the effluent combustion gases composed by the mixture of N_2, CO_2, and other gas are discharged through the production well [49]. It is well known that CO_2 can be dissolved into the heavy oil, and the light/middle components in the heavy oil are extracted into CO_2 rich phase, resulting in an volume swelling of heavy oil and a viscosity reduction [50, 51]. N_2 has a lower solubility in crude oil compared with CO_2, but N_2 has good expansion capability, which enables it to possess good ability of displacement, gas lift, drainage, and pressure maintenance during the exploitation stage. In addition, N_2 can enter the low-permeability interval that water cannot, to displace the bound crude oil, which further increases the crude oil production.

The flue gas in the Hongqian (H) NO. 1 wells area of Xinjiang Oilfield contains CO_2 of 10.0% to 15.0%, and N_2 of 80.0% to 85.0%. If the flue gas is directly discharged to the surroundings, it will inevitably result in waste of resources. Furthermore, CO_2 emission into the atmosphere will have a potential impact on the climate and environment, leading to the rising temperatures in the future [52, 53]. CO_2 is one of the main components causing the greenhouse effect, and decreasing the CO_2 content in the atmosphere is a key factor to mitigate the greenhouse effect. The negative impact of the greenhouse gas on the Earth's ecosystem, economic development, human health, and life quality cannot be ignored [54]. Therefore, the recycling of CO_2 and N_2 in the flue gas can not only save resources, but also achieve environmentally friendly production, helping to protect the atmospheric environment, and conforming to the concepts of green sustainable development plan.

This study aims to analyze the feasibility of flue gas reinjection and the resulting effect of asphaltene precipitation on the oilfield development. The precipitation pressure point test and X-ray energy spectrum were performed to show there mainly existed asphaltene precipitation. Then, through the flue gas injection by using the parallel double-pipe long-core, the displacement degree of high-permeability sandstone and low-permeability conglomerate reservoirs in WAG under different Gas–Water Ratio (GWR) was evaluated. Centrifugal capillary pressure and environmental scanning electron microscope experiments were used to determine the variations of petrophysical properties and precipitation morphology. The effects of precipitation on oil displacement and reservoir properties were analyzed and interpreted. In general, the investigation of the flue gas injection and its associated precipitation is of great significance in enhancing oil recovery and reducing environmental fingerprint by lowering greenhouse gas emission.

2 Samples

2.1 Formation oil and flue gas

In order to obtain basic data and results support for evaluating the feasibility of flue gas flooding and the impact of asphaltene on displacement of oil and petrophysical properties, a series of investigation on flue gas reinjection were carried out by injecting flue gas from H1 into the H48 fault reservoir. (Exempt H_2S and CO, other components of

the gas sample are consistent with the original flue gas). The formation oil was recombined with reference to the PVT parameters of the well from the H48 fault reservoir according to the National Standard GBT26981-2011 "Method for analyzing the fluid physical properties of oil and gas reservoirs", and it was recombined with separator oil (dead oil) of H118 well and synthesized solution gas (Required original solution gas on site is not available, so the synthesized solution gas was adopted). The PVT properties of recombined oil was verified by comparing the single-stage flash results between the recombined and original oil, to ensure its representativeness and provide qualified formation oil for subsequent experiments.

Forty liters of separator oil of H118 well were provided. The gas was synthesized with standard gases according to the original solution gas composition (Tab. A-1, shown in the Data in Brief). The single-stage flash results consisted of PVT parameters including GOR, volume coefficient, bubble point pressure, and crude oil viscosity and density etc. A comparison of the PVT properties between the recombined and original oil is shown in Table A-2 (shown in the Data in Brief). From the table, the properties of the recombined oil are generally consistent with the original PVT data of the latter one, which indicated good representativeness of the recombined oil.

The original flue gas composition contained little H_2S and CO which in all accounted for 1.6% of the overall composition. H_2S is highly toxic and CO is colorless, odorless, tasteless, and toxic. The effects of different flue gas compositions on displacement of oil are shown in Table A-3 (shown in the Data in Brief). Due to the low H_2S and CO content in the actual flue gas, the recovery without H_2S and CO is only 0.1% lower than that of the actual flue gas injection. Thus, to reduce the risk and improve the safety of the experiment, the content of H_2S and CO can be ignored in the subsequent experiments. Similar to the solution gas, the flue gas can be synthesized with standard pure gases in the laboratory. The molar composition of the synthesized flue gas was: 67.7% N_2, 13.9% CO_2, 0.9% O_2, 17.2% CH_4, 0.3% H_2.

2.2 Cores

More than 95.0% of the 1390 m ~ 1451 m sandstone and conglomerate cores in the H48 well were obtained at the beginning of the research, however, according to the test results, those cores could not meet the requirements due to the poor representativeness of porosity and permeability. Combined with the petrophysical properties of the actual H48 fault, 16 artificial cores (including 13 sandstones and 3 conglomerates) were adopted to replace the real cores for further tests. Before the starting of the experiment, six cores in the front, middle and back of the high-permeability (sandstone) and low-permeability (conglomerate) pipes were cut into four pieces each, and then the capillary pressure curve tests were performed before and after the displacement.

To simulate the effect of asphaltene on petrophysical properties, the cores are assembled with the decreasing permeability from the inlet to the outlet. From Tables A-4 and A-5 (shown in the Data in Brief), the total length of the combined sandstone cores in high-permeability pipe and conglomerate cores in low-permeability pipe is 79.1 cm and 74.8 cm respectively, with the average permeability of 139.4 mD and 42.5 mD, and the pore volume of 388.1 mL and 825.7 mL respectively.

2.3 Formation water

The formation water was obtained according to the analysis report of original formation water in H118 Well. From Table A-6 (shown in the Data in Brief), the main component of water was $NaHCO_3$ with the total salinity of 13 913.7 mg/L.

3 Experimental research

3.1 Precipitation pressure test

There was high asphaltene content in the recombined oil of research block. The mutual mass transfer occurred between injected gas and the oil, and may destroy the equilibrium state of the oil, which could result in the precipitation. It was evaluated whether precipitation occurred during the flue gas reinjection by laser method to determine the precipitation pressure point. The density of oil decreased as the pressure decreased because the pressure was kept above the bubble point pressure, so the laser light transmission intensity gradually increased. However, when the precipitation occurred, its scattering effect on the laser light dominated and the received laser intensity decreased. Thus, the pressure at which the power of receiver started to decrease was defined as the precipitation pressure.

Before the laser test, five bubble point pressure tests of the oil under different amounts of gas injection (0.0 mol%, 2.0 mol%, 4.0 mol%, 8.0 mol%, 13.0 mol%) were performed: the pressurized flue gas was injected into the recombined oil which was stabilized at the formation temperature of 42 °C for 2 h, and then fully stirred until it was a homogeneous single-phase; the pressure of oil was slowly reduced to measure its bubble point pressure; the above steps were repeated to complete five tests. The experimental flow chart is shown in Figure A-1 (shown in the Data in Brief).

Similarly, five precipitation pressure point tests under different amounts of gas injection were carried out respectively, as shown in Figure A-2 (shown in the Data in Brief): the flue gas was pressurized to 30.0 MPa or 40.0 MPa and transferred into the oil; then the pressure was gradually reduced and it was ensured that the pressure was always higher than bubble point pressure during the process; after the oil-phase and pressure were both stable, the power of laser receiver was recorded at this time; the above steps were repeated until five tests were completed.

3.2 Demonstration of precipitation component

After the laser test, the pressure was raised to the current formation pressure of 10.0 MPa. The oil with 13.0 mol% gas injection was filtered by three filter papers with 1.2 μm diameter and the remaining precipitation was analyzed by environmental scanning electron microscope and X-ray energy spectrum. Generally, precipitation in crude oil mainly includes wax and asphaltene. The wax is mostly

composed of alkane with the dominant normal paraffin content and a small amount of isoparaffin and naphthenes. Asphaltene is a complex mixture composed of macromolecular hydrocarbons and their non-metallic derivatives, containing some O, S, N, Cl, and a few metallic ionic elements [55]. Thereby, it could be confirmed that the precipitation contained asphaltene as long as O, S, N, Cl, or metallic elements were determined by energy spectrum analysis.

3.3 Study on flue gas injection and precipitation in parallel long core

The displacement device consists of an injection system, a core holder system and a production system, as shown in Figure A-3 (shown in the Data in Brief). The formation water was injected into the high-permeability pipe and the low-permeability pipe simultaneously. Then the pressure was raised to the original formation pressure of 15.0 MPa and the saturated water volume of each core was recorded. The recombined live oil is used to displace the water out of cores located in the high-permeability and the low-permeability pipes respectively, to establish the irreducible water saturation. With the steady GOR at the outlet, the oil-phase permeability of the sandstone and conglomerate are measured as K_{1-1} and K_{2-1}, respectively.

The production process of the reservoir was simulated based on WAG to improve the sweep efficiency of the heterogeneous reservoir. The pressure was reduced to the current formation pressure of 10.0 MPa, and then WF was carried out at a constant velocity (0.1 mL/min). When the water cut of the high-permeability pipe reached 98.0%, four tests of WAG at different GWR values (water slug size: 0.1 HCPV; GWR: 1:1, 2:1, 3:1, 4:1) were performed. The injection rate is consistent with the WF's, and the volume of injection fluid, production oil and gas, and pressure difference are recorded. After WAG was finished, the solution gas was injected into the high-permeability and low-permeability pipes, and the core pressure was raised to the original formation pressure 15.0 MPa. Then, the recombined oil was used to displace the fluid in the cores until GOR at the outlet was steady, and the oil-phase permeability K_{1-2} and K_{2-2} were tested respectively. After one test was finished, the cores were washed with petroleum ether and absolute alcohol, and the next test was repeated at different gas/water ratios. All the cores were washed with toluene before the 4th test to see if toluene can relieve the asphaltene.

After four tests were all finished, the inlet, middle, and outlet cores were taken, washed with petroleum ether, dried, and weighed. The precipitation content in the core was determined by measuring the weight difference before and after the experiments. The precipitation saturation was estimated by reference to the asphaltene density and the pore volume of each core.

3.4 Effect of precipitation on microscopic pore structure

The capillary pressure curve is one of the important parameters for characterizing the microscopic pore structure of porous media. In order to better characterize the capillary pressure of the core, the capillary pressure curves of all the cores in the high-permeability and low-permeability pipes were measured by centrifugation [56] before and after flue gas injection. The main equipment includes: TG1850-WS centrifuge, HJT-200 g electronic balance, vacuum pump, interface tensiometer, etc. Usually, the core diameter is 2.5 cm ~ 3.8 cm, and the length is 2.5 cm ~ 5.0 cm. The

Table 1. Bubble point pressure under different amounts of gas injection.

Gas injection/mol%	P_b/MPa
0.0	10.5
2.0	13.1
4.0	15.5
8.0	19.8
13.0	30.5

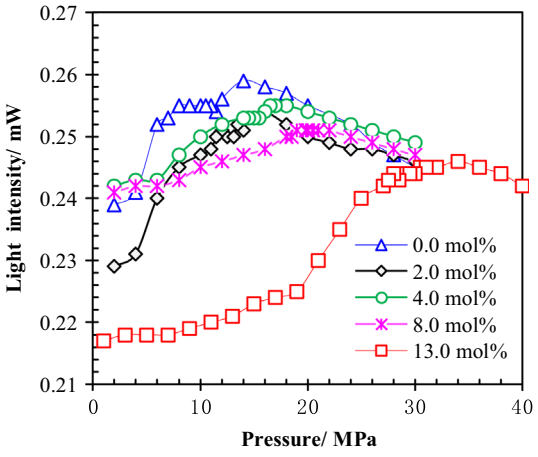

Fig. 1. Precipitation pressure tests under different amounts of gas injection.

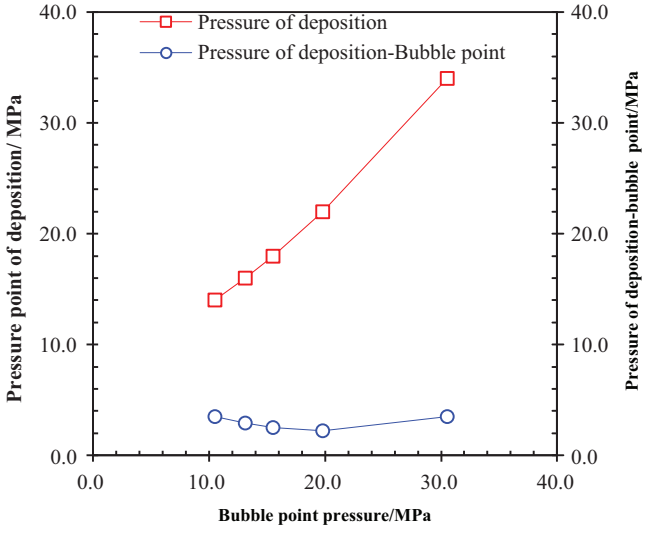

Fig. 2. Relationship between bubble point pressure and precipitation pressure under different gas injections.

Table 2. Energy spectrum and scanning electron microscope analysis.

Number	Energy spectrum	Scanning electron microscope
1	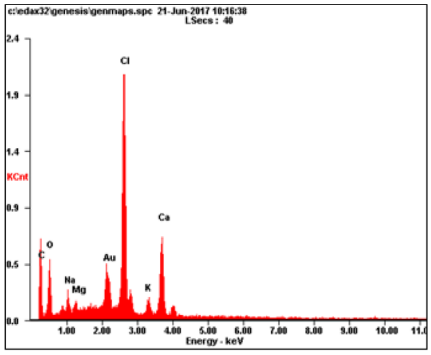	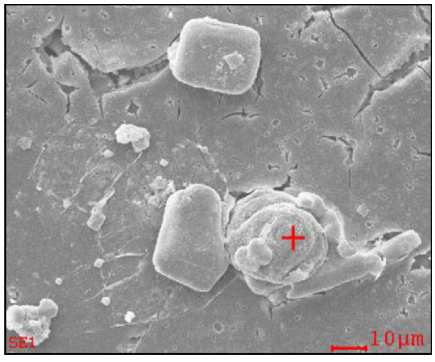
2	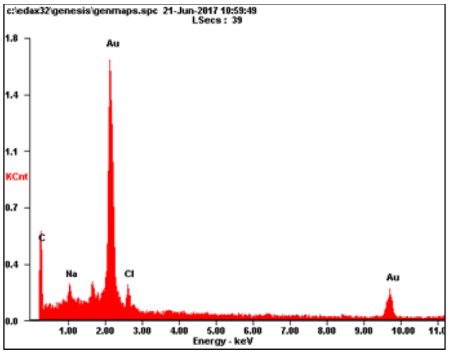	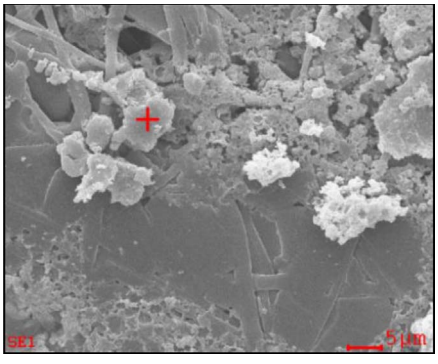
3	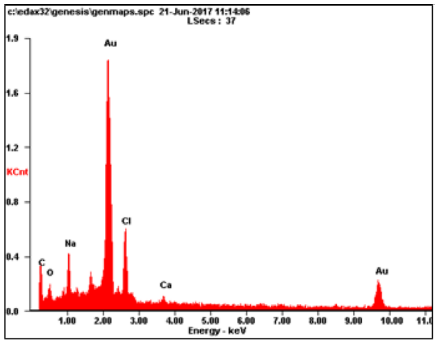	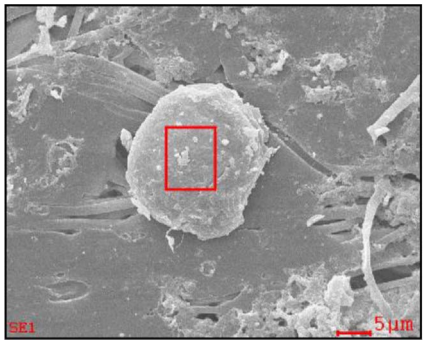

cores were washed and dried before the experiments to measure the permeability and porosity.

Quanta 450 environmental scanning electron microscope by American *FEI Company* was used for observing the precipitation morphology in cores. The size of cores is compatible with the instrument with the height of about 5.0 mm ~ 10.0 mm. The cores were treated by ion sputtering to avoid charge accumulation affecting image quality, and thermal damage. The cores were evacuated in the electron microscope, and then its truncation surfaces were scanned to observe the results.

4 Results

4.1 Results of precipitation pressure test

Table 1 showed the more gas was injected, the higher the bubble point pressure of the oil. The results of precipitation pressure test were shown in Figure 1 (the precipitation pressure is where the light intensity of receiver started to decrease): the bubble point pressure and precipitation pressure were 10.5 MPa and 14.0 MPa respectively for 0.0 mol%, 13.1 MPa and 16.0 MPa for 2.0 mol%, 15.5 MPa and

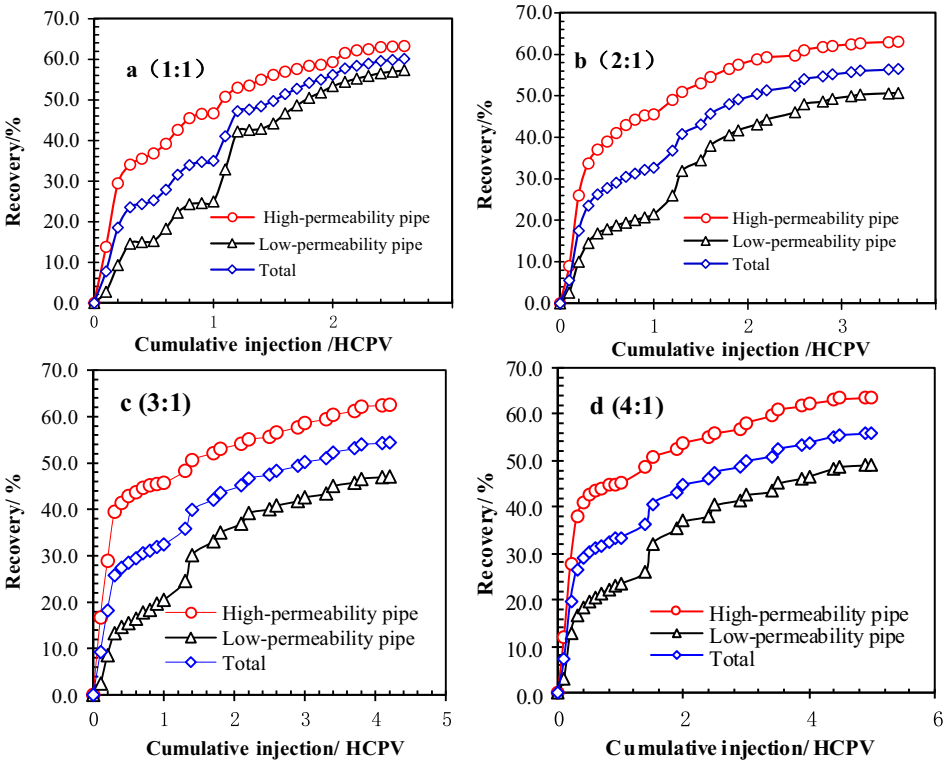

Fig. 3. (a–d) Recovery-cumulative injection for combining WF and WAG.

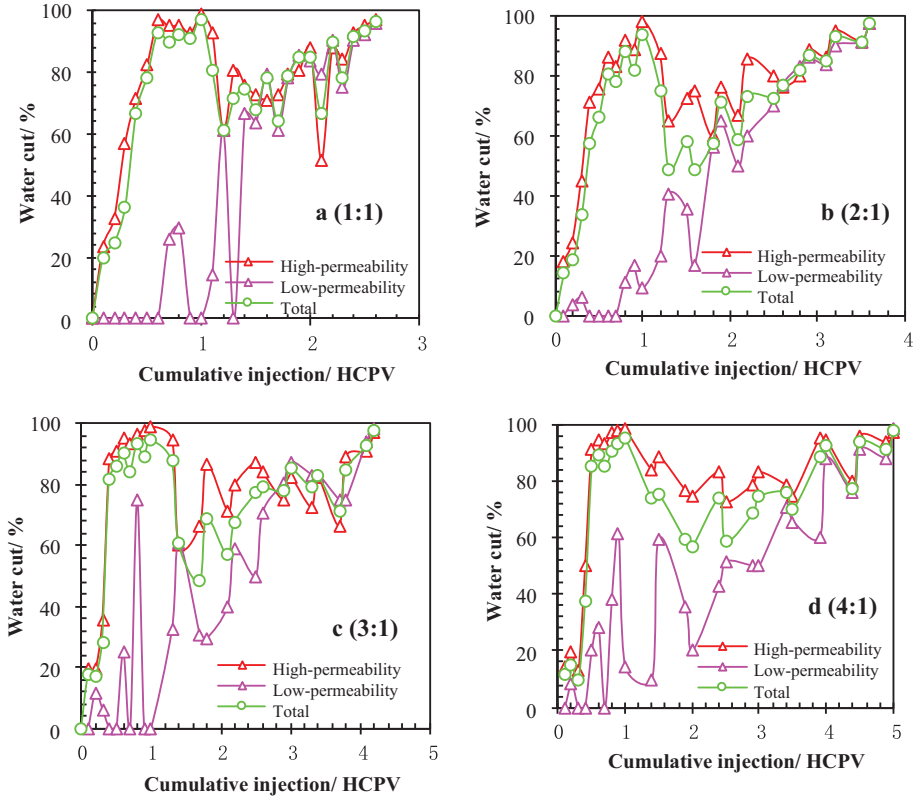

Fig. 4. (a–d) Water cut-cumulative injection for combining WF and WAG.

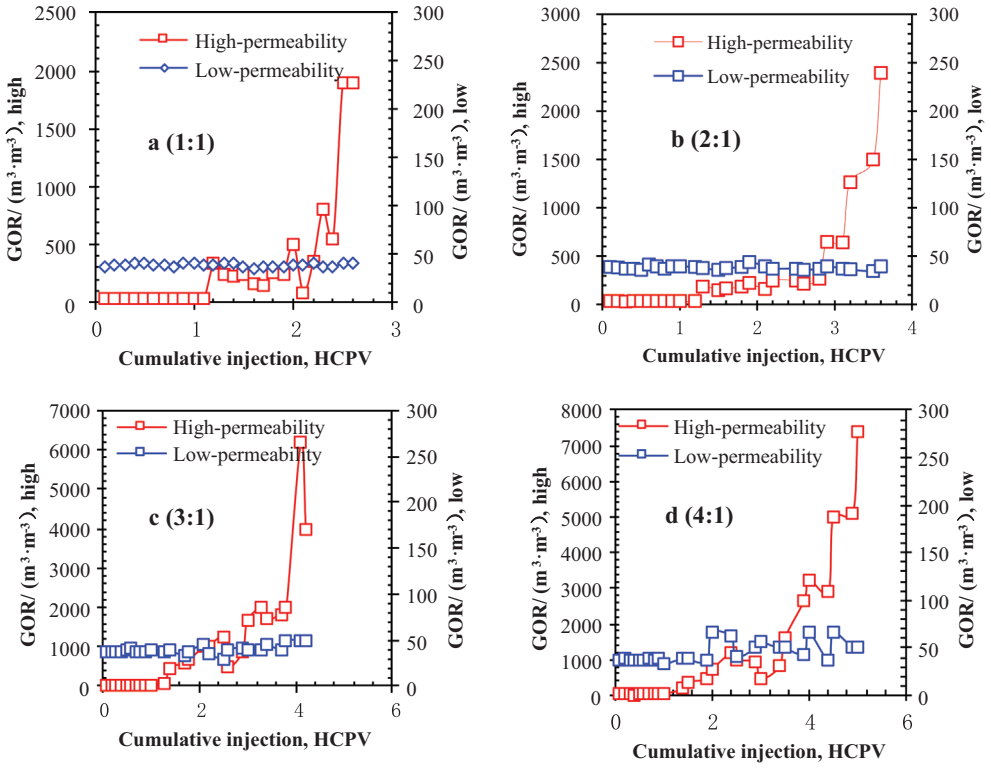

Fig. 5. (a–d) GOR-cumulative injection for combining WF and WAG.

Table 3. Reduction degree of permeability (high-permeability).

GWR		Flow rate (mL/30 min)	Pressure difference (psi)	Permeability (mD)	Reduction degree (%)
1:1	K_{1-1}	4.2	40	129.9	38.1
	K_{1-2}	3.9	60	80.4	
2:1	K_{1-1}	4.1	45	112.7	46.5
	K_{1-2}	3.9	80	60.3	
3:1	K_{1-1}	5.1	70	90.1	56.5
	K_{1-2}	3.8	120	39.2	
4:1	K_{1-1}	4.2	45	115.5	30.4
	K_{2-2}	3.9	60	80.4	

K_{1-1}: before WAG; K_{1-2}: after WAG.

Table 4. Reduction degree of permeability (low-permeability).

GWR		Flow rate (mL/30 min)	Pressure difference (psi)	Permeability (mD)	Reduction degree (%)
1:1	K_{2-1}	5.6	70	41.6	46.9
	K_{2-2}	5.1	120	22.1	
2:1	K_{2-1}	5.4	80	35.1	51.9
	K_{2-2}	5.2	160	16.9	
3:1	K_{2-1}	5.3	90	30.6	61.5
	K_{2-2}	5.1	225	11.8	
4:1	K_{2-1}	6.2	90	35.8	45.3
	K_{2-2}	4.9	130	19.6	

K_{2-1}: before WAG; K_{2-2}: after WAG.

Table 5. Precipitation saturation of cores after displacement.

High-permeability (sandstone)				Low-permeability (Conglomerate)			
Core number	Before/g	After/g	Saturation%	Core number	Before/g	After/g	Saturation%
38 (inlet)	66.25	66.28	0.7	12	25.18	25.21	1.8
19 (middle)	66.93	66.98	1.1	19	24.38	24.42	2.4
23 (outlet)	67.22	67.35	2.7	5	24.16	24.26	5.3

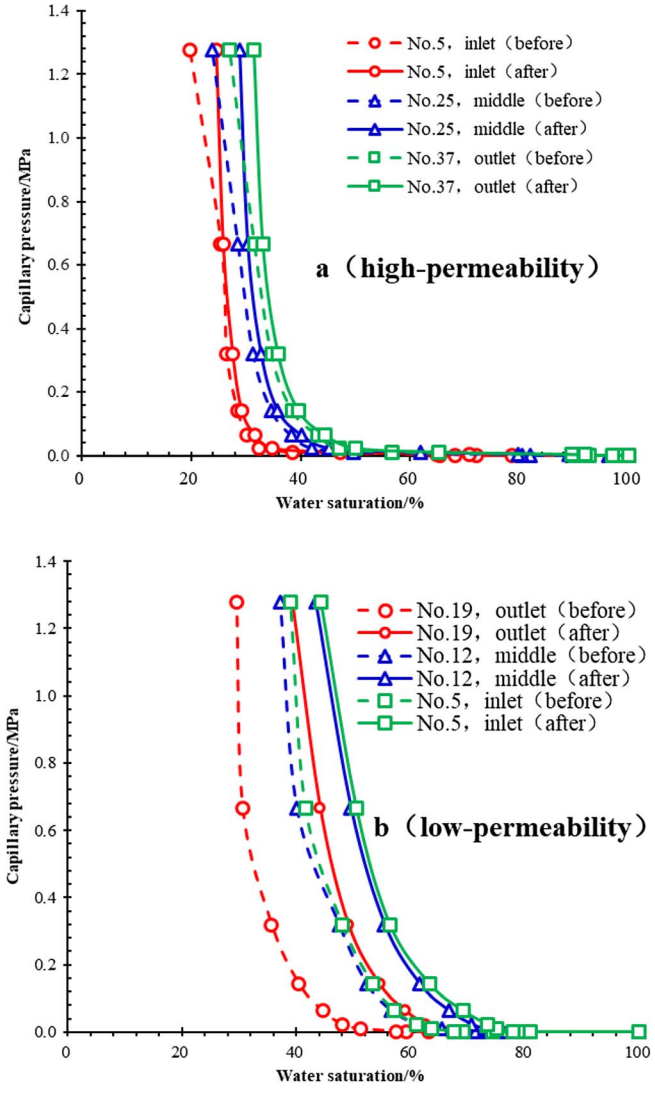

Fig. 6. (a and b) Comparison of capillary pressure before and after WAG.

18.0 MPa for 4.0 mol%, 19.8 MPa and 22.0 MPa for 8.0 mol%, 30.5 MPa and 34.0 MPa for 13.0 mol%. According to Figure 2, the precipitation pressure rised with the increase of the amount of gas injection, generally 2.0 MPa ~ 3.0 MPa higher than the bubble point pressure.

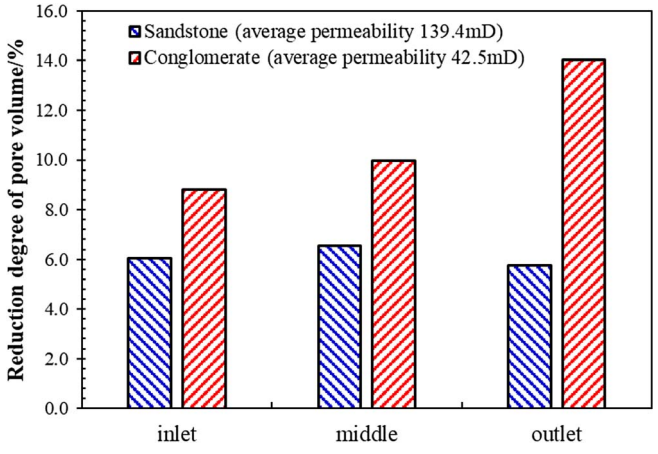

Fig. 7. Reduction degree of pore volume after WAG.

4.2 Demonstration result of precipitation component

According to Table 2, the precipitation particles mainly contained C, N, O, Cl elements: the content of C element is 89.3 wt% ~ 48.2 wt%, 3.6 wt% ~ 15.7 wt% of O element, 17.2 wt% ~ 21.8 wt% of N element, 3.8 wt% ~ 17.8 wt% of Cl element, and a small amount of metallic elements was also contained such as Na, Au, K, and Mg. Combined with the characteristics of asphaltene composition and the ionic elements, it can be confirmed that the precipitation generated during the flue gas reinjection was mainly asphaltene.

4.3 Study on flue gas injection and precipitation in parallel long core

The experimental process was divided into three stages: pressure depletion, WF and WAG. Due to the low preliminary recovery in the pressure depletion stage (2.8% ~ 2.9%), mainly the WF and WAG are analyzed.

4.4 The results of WAG

WF: 1 HCPV of formation water was cumulatively injected during the WF period. As shown in Figures 3a–3d, the oil recovery in high-permeability and low-permeability pipes at different GWR are 45.2% ~ 46.7% and 20.5% ~ 24.9% respectively, with the total recovery of 32.4% ~ 34.9%. As indicated by Figures 4a–4d, the water injected during WF mainly flowed through the layer with high permeability,

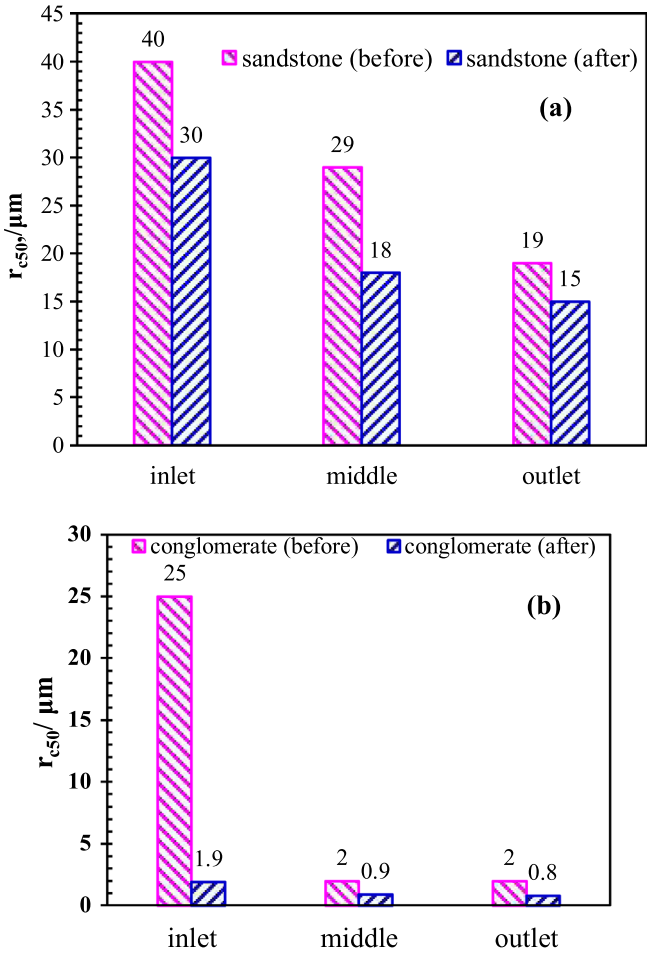

Fig. 8. (a and b) Comparison of r_{c50} before and after WAG.

and the total water cut is close to the layer's with high permeability.

WAG: WAG was performed following the WF process. When WAG was finished, as shown in Figures 3a–3d, the oil recovery at different GWR in high-permeability pipe are: 63.3% (1:1), 63.9% (2:1), 62.6% (3:1), 63.7% (4:1), while the recovery in low-permeability pipe are: 57.3% (1:1), 50.7% (2:1), 47.1%. (3:1), 49.3% (4:1), and the total recovery is: 54.5% ~ 60.0%. The variation of GWR had slight effect on the recovery of high-permeability pipe, while the recovery of low-permeability pipe decreased significantly with the increase of GWR. The recovery in high-permeability pipe increased by 16.6% (1:1), 18.4% (2:1), 16.9% (3:1), 18.6% (4:1) and in low-permeability pipe increased by 32.4% (1:1), 29.3% (2:1), 26.6% (3:1), 25.7% (4:1), and the total recovery increased by 22.0% ~ 25.1%. The recovery of low-permeability pipe had been improved more greatly due to the better volumetric sweep efficiency from the WAG process. From Figures 4a–4d, compared with WF, WAG can alleviate the problem of turbulent injected water through the high-permeability pipe and increase the sweep volume of water in the low-permeability, which greatly reduced the water cut in high-permeability pipe and total water cut, and improved the displacement efficiency of oil.

Since the injected gas flowed quickly through the layer with high permeability (Figs. 5a–5d), the gas breakthrough occurred with the cumulative injection of 0.6 HCPV (1:1), 1.2 HCPV (2:1), 0.6 HCPV (3:1), 0.8 HCPV (4:1) of flue gas injection, respectively; and the GOR reached 350 m^3/m^3 (1:1), 650 m^3/m^3 (2:1), 600 m^3/m^3 (3:1), 720 m^3/m^3 (4:1) at the gas breakthrough respectively. The GOR in the layer with low permeability did not vary significantly in the absence of gas breakthrough.

4.5 Effect on the rock permeability

The results of permeability tests are shown in Tables 3 and 4. The permeability variations of low-permeability and high-permeability pipes all reached the maximum values at the GWR of 3:1, with the reduction degree of 61.5% and 56.5%, respectively. After the cleaning of rock with toluene, for the 4th test, the permeability reduction degree in low-permeability and high-permeability pipes was 45.3% and 30.4%, which indicated that to some extent toluene can relieve the asphaltene in the core.

4.6 Test results of precipitation saturation

From Table 5, the saturation of precipitation on sandstone cores in high-permeability pipe and conglomerate cores in low-permeability pipe is 0.7% ~ 2.7% and 1.8% ~ 5.3% respectively. For the cores with the same lithology, the precipitation saturation increased from the inlet to the outlet.

4.7 Effect of precipitation on microscopic pore structure of rocks

4.7.1 Test results of pore structure

The comparison of the capillary pressure curves for six cores before and after experiments are shown in Figures 6a and 6b. Normally, the increase of capillary pressure is caused by pore radius reduction or the wettability alteration from oil-wet to water-wet. However, the asphaltene on the rock surface will lead to the wettability alteration from water-wet to oil-wet [57, 58], so in this research the wettability can be excluded out of the influencing factors of the increase of capillary pressure, and pore radius was considered. The capillary pressure curve after the displacement is above the capillary pressure curve before the displacement, indicating that the capillary pressure increased with the decrease of pore radius during the WAG.

The reduction degree of pore volume could be deduced according to the change of the irreducible water saturation, as shown in Figure 7. The reduction degree of pore volume for sandstone is 5.9% ~ 6.6% with an average of 6.2%, and for conglomerate is 8.7% ~ 13.9% with an average of 10.8%, which was mainly caused by the decrease of pore radius and indicated a more significant effect on the pore volume of conglomerate.

According to the characteristics of the capillary pressure curve, the median radius of capillary pressure corresponding to the core was calculated by the capillary median pressure ($P_{c50} = 2\sigma\cos\theta/r_{c50}$), as shown in Figures 8a and 8b. The median radius of capillary pressure of sandstone before

Table 6. Microscopic characteristics of precipitation.

Number	Morphology	Characteristics	Corresponding cores
1	Pore filling of agglomerated particles	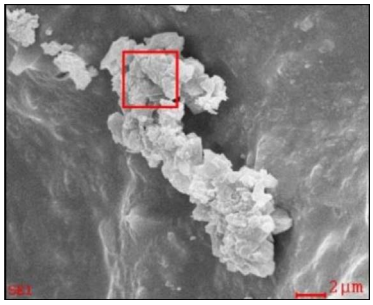	All cores
2	Precipitation of isolated particles on pore surface	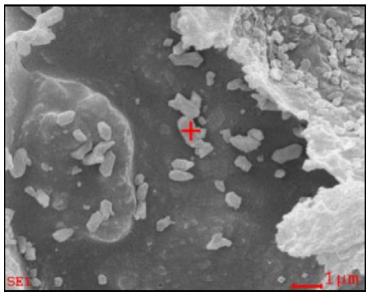	All cores
3	Film-like coverage of small particles	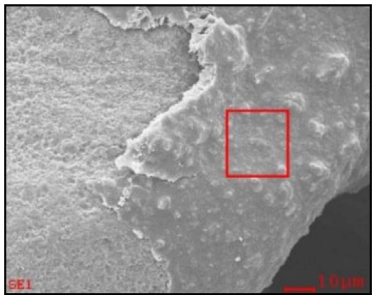	Conglomerate

experiment was 19–40 μm and after experiment was 15–28 μm with the reduction degree of 28.0%. Due to the strong heterogeneity of the conglomerate, big reduction degree of 60.0% ~ 92.4% in the median radius of capillary pressure was noticed.

4.7.2 Test results of surface microscopic characteristics

The rock samples have a certain randomness, but it does not affect the statistical analysis. As the results of scanning electron microscope (Tab. 6) showed, the retention mechanisms of solid-phase particles in cores after WAG are mainly surface precipitation, pore throat plugging and pore filling, and film-like particles deposition.

5 Discussion

The content of the middle-hydrocarbon component of the oil including C_2–C_6 and C_{11+} decreased with more gas injection, which resulted in the decrease of solubility to precipitation and the precipitation occurred earlier. Thus, the precipitation pressure rised with more gas injection, generally 2.0 MPa ~ 3.0 MPa higher than the bubble point pressure.

According to Figure 9, the average increase degree of recovery for the low-permeability layer after WAG is 28.5%, which is much higher than the average of high-permeability layer of 17.4%. Thus, the key factor controlling the efficiency of WAG is the displacement degree of reserve with low permeability. The increase degree of recovery for the low-permeability layer was the largest at the GWR 1:1 and gradually decreased from 32.4% to 25.7% with the increasing GWR. From the results of permeability test, the decrease degree of permeability for all the cores also increased with higher GWR. The average recovery of the four tests after WF is 33.4% and after WAG is 56.8% with the average enhanced recovery of 23.4%. Thus, the WAG technology after WF has a promising prospect for future application and popularization.

The capillary pressure curve after the displacement is above that before the displacement, indicating the increase

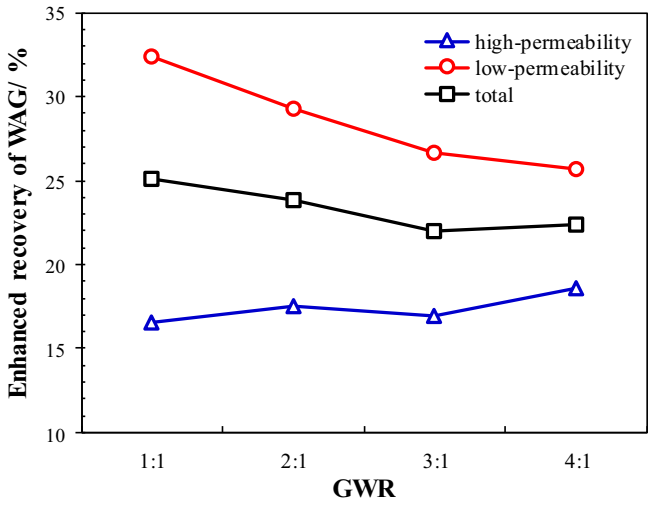

Fig. 9. Comparison of enhanced recovery of WAG at different GWR.

of capillary pressure resulting from the decrease of pore radius caused by precipitation block. The precipitation occupied some pores, which resulted in the decrease of median radius of capillary pressure and effective porosity in all cores with more impacts in the low-permeability pipes. For the cores with the same lithology, the precipitation was strengthened significantly as the permeability decreased from the inlet to the outlet. Meanwhile, the test of precipitation saturation also proved the same results, indicating that the worse the petrophysical properties (e.g., the lower original permeability), the easier it is to retain the precipitation.

6 Conclusion

The results of five laser tests showed that as the amount of gas injection increased, the precipitation pressure rised, generally 2.0 MPa ~ 3.0 MPa higher than the bubble point pressure. Scanning electron microscope and energy spectrum analysis showed that the precipitation was mainly asphaltene. The test results of precipitation saturation, and the reduction degree of effective porosity and median radius of capillary pressure from the capillary pressure curve showed that for the cores with the same lithology, they gradually increased with poorer petrophysical properties from the inlet to outlet. The impact of precipitation on the conglomerate was severer than that on sandstone. In summary, the poorer the petrophysical properties, the easier it is to retain precipitation and the greater the effect of precipitation. From the results of scanning electron microscope, the precipitation morphology included the agglomerated particles filling in the pores, the isolated particles deposition on the surface and film-like asphaltene.

During the displacement, the injected fluid mainly flowed through the high-permeability layer and the total water cut and GOR are close to those out of the high-permeability layer. The key factor affecting efficiency of WAG is the displacement degree of reserve with the low permeability. The average enhanced recovery of the low-permeability layer is 28.5%, much higher than that of the high-permeability layer 17.4%. During WAG, the increasing GWR resulted in the higher decrease degree of recovery in the low-permeability layer and slight change of recovery in high-permeability layer, and the optimum GWR should be 1:1. The average recovery of the four tests after WF is 33.4%, and after WAG is 56.8% with the enhanced recovery of 23.4%. In general, the WAG could greatly improve the recovery after WF. However, the precipitation has a significant impact on the petrophysical properties. Thus, the influence of precipitation must be considered when the gas injection program is formulated.

Data availability

Some or all data, models, or code that support the findings of this study are available from the corresponding author upon reasonable request.

Funding sources

This work was supported by *National Natural Science Foundation of China* (5183000045), *National Major Science and Technology Project of CNPC* "Research and Application of Key Technologies for Benefit Development of Volcanic Rock Reservoirs" (2017E-04-05), *and Sichuan Province Science and Technology Support Program* (2019YFG0457).

Acknowledgments. The *National Natural Science Foundation* greatly provides the financial support for this research. Songhai Qing is acknowledged for his assistance in collecting experimental data.

Supplementary materials

Supplementary material is available at https://ogst.ifpenergiesnouvelles.fr/10.2516/ogst/2020041/olm

Table A-1. Comparison of molar composition between synthesized and original solution gas.

Table A-2. Comparison of single-stage flash results between recombined and original oil.

Table A-3. Comparison of oil displacement efficiency of different flue gas composition cases.

Table A-4. Physical properties and order of cores.

Table A-5. Physical properties and order of cores.

Table A-6. Analysis of formation water in H118 well.

Fig. A-1. Comprehensive schematic diagram of PVT properties and precipitation pressure tests.

Fig. A-2. Flow chart of laser tests.

Fig. A-3. Flow chart of long-core experiment.

References

1 Jia B., Tsau J.S., Barati R. (2019) A review of the current progress of CO_2 injection and carbon storage in shale oil reservoirs, *Fuel* **236**, 404–427.

2 Hustad O.S., Holt T. (1992) Gravity stable displacement of oil by hydrocarbon gas after waterflooding, in: *Paper SPE 24116 Presented at the SPE/DOE Eighth Symposium on Enhanced Oil Recovery, Tulsa, Oklahoma, 22–24 April*.

3 Donaldson, E.C., Chilingarian G.V. (2009) *Enhanced Oil Recovery, II: Processes and Operations* (Developments in Petroleum Science), Elsevier Science Ltd. ISBN: 9780444429339.

4 Kulkarni M.M., Rao D.N. (2005) Experimental investigation of miscible and immiscible water-alternating-gas (wag) process performance, *J. Pet. Sci. Eng.* **48**, 1–2, 1–20.

5 Pariani G.J., McColloch K.A., Warden S.L., Edens D.R. (1992) An approach to optimize economics in a west Texas CO_2 flood, *J. Pet. Technol.* **44**, 9, 984.

6 Chen B., Reynolds A.C. (2016) Ensemble-based optimization of the water-alternating-gas-injection process, *SPE J.* **21**, 3, 786–798.

7 Kulkarni M.M., Rao D.N. (2004) Experimental investigation of various methods of tertiary gas injection, in: *SPE Annual Technical Conference and Exhibition, 26–29 September, Houston, Texas*.

8 Changlin-lin L., Xin-wei L., Xiao-liang Z., Ning L., Hong-na D., Huan W., Yong-ge L. (2013) Study on enhanced oil recovery technology in low permeability heterogeneous reservoir by water-alternate-gas of CO_2 flooding, in: *SPE Asia Pacific Oil and Gas Conference and Exhibition, 22–24 October, Jakarta, Indonesia*.

9 Pariani G.J., McColloch K.A., Warden S.L., Edens D.R. (1992) An approach to optimize economics in a west Texas CO_2 flood, *J. Pet. Technol.* **44**, 9, 984–1025.

10 Afzali S., Rezaei N., Zendehboudi S. (2018) A comprehensive review on enhanced oil recovery by water alternating gas (wag) injection, *Fuel* **227**, 218–246.

11 Tabzar A., Fathinasab M., Salehi A., Bahrami B., Mohammadi A.H. (2018) Multiphase flow modeling of asphaltene precipitation and deposition, *Oil Gas Sci. Technol. - Rev. IFP Energies nouvelles* **73**, 3, 51.

12 Huang E.T.S. (1992) The effect of oil composition and asphaltene content on CO_2 displacement, in: *Presented at the SPE/DOE Eighth Symposium on Enhanced Oil Recovery, 22–24 April, Tulsa, OK*. Paper SPE 24131.

13 Hamadou R., Khodja M., Kartout M., Jada A. (2008) Permeability reduction by asphaltenes and resins deposition in porous media, *Fuel* **87**, 10–11, 2178–2185.

14 Collins S., Melrose J. (1983) In adsorption of asphaltenes and water on reservoir rock minerals, in: *SPE Oilfield and Geothermal Chemistry Symposium, 1–3 June, Denver, Colorado*.

15 Clementz D. (1982) In alteration of rock properties by adsorption of petroleum heavy ends: Implications for enhanced oil recovery, in: *Paper SPE 10683, SPE, DOE Symposium on Enhanced Oil Recovery, Tulsa, 4–7 April*.

16 González G., Moreira M.B.C. (1991) The wettability of mineral surfaces containing adsorbed asphaltene, *Colloids Surf.* **58**, 3, 293–302.

17 Al-Maamari R.S.H., Buckley J.S. (2003) Asphaltene precipitation and alteration of wetting: the potential for wettability changes during oil production, *SPE Reserv. Evalu. Eng.* **6**, 4, 210–214.

18 Soorghali F., Zolghadr A., Ayatollahi S. (2014) Effect of resins on asphaltene deposition and the changes of surface properties at different pressures: A microstructure study, *Energy Fuels* **28**, March–April, 2415–2421.

19 Borton D., Pinkston D.S., Hurt M.R., Tan X., Azyat K., Scherer A., Tykwinski R., Gray M., Qian K., Kenttämaa H.I. (2010) Molecular structures of asphaltenes based on the dissociation reactions of their ions in mass spectrometry, *Energy Fuels* **24**, September–October, 5548–5559.

20 Andersen S. (1994) Effect of precipitation temperature on the composition of n-heptane asphaltenes, *Liq. Fuels Technol.* **12**, 1, 51–74.

21 Kim S.T., Boudh-Hir M.E., Mansoori G.A. (1990) The role of asphaltene in wettability reversal, in: *SPE Annual Technical Conference and Exhibition, 23–26 September, New Orleans, Louisiana*.

22 Buckley J.S., Wang J. (2002) Crude oil and asphaltene characterization for prediction of wetting alteration, *J. Pet. Sci. Eng.* **33**, 1, 195–202.

23 Mansoori G.A. (1997) Modeling of asphaltene and other heavy organic depositions, *J. Pet. Sci. Eng.* **17**, 101–111.

24 Pacheco-Sanchez J.H., Ali Mansoori G. (1998) Prediction of the phase behavior of asphaltene micelle/aromatic hydrocarbon systems, *Pet. Sci. Technol.* **16**, 3–4, 377–394.

25 Speight J.G. (1980) The chemistry and technology of petroleum, *Appl. Catal.* **2**, 6, 406–407.

26 Mitchell D.L., Speight J.G. (1973) The solubility of asphaltenes in hydrocarbon solvents, *Fuel* **52**, 2, 149–152.

27 Speight J.G., Long R.B., Trowbridge T.D. (1984) Factors influencing the separation of asphaltenes from heavy petroleum feedstocks, *Fuel* **63**, 5, 616–620.

28 Yen T.F., Erdman J.G., Pollack S.S. (1961) Investigation of the structure of petroleum asphaltenes by x-ray diffraction, *Anal. Chem.* **33**, 11, 1587–1594.

29 Alomair O.A., Almusallam A.S. (2013) Heavy crude oil viscosity reduction and the impact of asphaltene precipitation, *Energy Fuels* **27**, 12, 7267–7276.

30 Yen A., Yin Y.R., Asomaning S. (2001) Evaluating asphaltene inhibitors: Laboratory tests and field studies, in: *Paper SPE 65376-MS presented at the SPE International Symposium on Oilfield Chemistry, 13–16 February, Houston, Texas*.

31 Vazquez D., Mansoori G.A. (2000) Identification and measurement of petroleum precipitates, *J. Pet. Sci. Eng.* **26**, 49–55.

32 Zanganeh P., Ayatollahi S., Alamdari A., Zolghadr A., Kord S. (2011) Asphaltene deposition during CO_2 injection and pressure depletion: a visual study, *Energy Fuels* **25**, 753–761.

33 Speight J.G. (1996) Asphaltenes: Fundamentals and applications by E.Y. Sheu and O.C. Mullins. Plenum Press, New York, 1995; 236 pages plus index. $79.50. ISBN No. 0-306-45191-3, *Liq. Fuels Technol.* **14**, 10, 1475.

34 Leontaritis K.J., Mansoori G.A. (1988) Asphaltene deposition: A survey of field experiences and research approaches, *J. Pet. Sci. Eng.* **1**, 3, 229–239.

35 Hashemi-Kiasari H., Hemmati-Sarapardeh A., Mighani S., Mohammadi A.H., Sedaee-Sola B. (2014) Effect of operational parameters on SAGD performance in a dip heterogeneous fractured reservoir, *Fuel* **122**, April, 32–93.

36 Idem R.O., Ibrahim H.H. (2002) Kinetics of CO_2-induced asphaltene precipitation from various saskatchewan crude oils during CO_2 miscible flooding, *J. Pet. Sci. Eng.* **35**, 3, 233–246.

37 Abdallah D., Al-Basry A., Zwolle Z., Grutters M., Huo Z., Stankiewicz A. (2010) Asphaltene studies in on-shore Abu Dhabi oil fields. Part II: Investigation and mitigation of asphaltene deposition – A case study, in: *Paper SPE 138039-MS Presented at the Abu Dhabi International Petroleum*

Exhibition and Conference, 1–4 November 2010, Abu Dhabi, UAE.

38 Eskin D., Mohammadzadeh O., Akbarzadeh K., Taylor S.D., Ratulowski J. (2016) Reservoir impairment by asphaltenes: A critical review, *Can. J. Chem. Eng.* **94**, 6, 1202–1217.

39 Leontaritis K.J., Mansoori G.A. (1988) Asphaltene deposition: A survey of field experiences and research approaches, *J. Pet. Sci. Eng.* **1**, 3, 229–239.

40 Gonzalez D.L., Mahmoodaghdam E., Lim F.H., Joshi N.B. (2012) Effects of gas additions to deepwater gulf of mexico reservoir oil: Experimental investigation of asphaltene precipitation and deposition, in: *SPE Annual Technical Conference and Exhibition, 8–10 October, San Antonio, Texas, USA*.

41 Meng X. (2017) *Experimental and numerical study of enhanced condensate recovery by gas injection in shale gas-condensate reservoirs*, Society of Petroleum Engineers. doi: 10.2118/183645-PA.

42 Shen Z., Sheng J.J. (2018) Experimental and numerical study of permeability reduction caused by asphaltene precipitation and deposition during CO_2 huff and puff injection in eagle ford shale, *Fuel* **211**, January 1, 432–445.

43 Fakher S., Imqam A. (2019) Asphaltene precipitation and deposition during CO_2 injection in nano shale pore structure and its impact on oil recovery, *Fuel* **237**, 1029–1039.

44 Srivastava R.K., Huang S.S., Dong M. (1999) Asphaltene deposition during CO_2 flooding, *SPE Prod. Facil.* **14**, 4, 235–245.

45 Ashoori S., Balavi A. (2014) An investigation of asphaltene precipitation during natural production and the CO_2 injection process, *Pet. Sci. Technol.* **32**, 11, 1283–1290.

46 Behbahani T.J., Ghotbi C., Taghikhani V., Shahrabadi A. (2012) Investigation on asphaltene deposition mechanisms during CO_2 flooding processes in porous media: A novel experimental study and a modified model based on multilayer theory for asphaltene adsorption, *Energy Fuels* **26**, 8, 5080–5091.

47 Takahashi S., Hayashi Y., Takahashi S., Yazawa N., Sarma H. (2003) In characteristics and impact of asphaltene precipitation during CO_2 injection in sandstone and carbonate cores: An investigative analysis through laboratory tests and compositional simulation, in: *SPE International Improved Oil Recovery Conference in Asia Pacific, 20–21 October, Kuala Lumpur, Malaysia*.

48 Shedid S.A., Zekri A.Y. (2006) Formation damage caused by simultaneous sulfur and asphaltene deposition, *SPE Prod. Oper.* **21**, 1, 58–64.

49 Ado M.R., Greaves M., Rigby S.P. (2018) Effect of pre-ignition heating cycle method, air injection flux, and reservoir viscosity on the THAI heavy oil recovery process, *J. Pet. Sci. Eng.* **166**, S0920410518302195.

50 Sayegh S.G., Maini B.B. (1984) Laboratory evaluation of the CO_2 huff-n-puff process for heavy oil reservoirs, *J. Can. Pet. Technol.* **23**, 3, 29–36.

51 Simpson M.R. (1988) The CO_2 huff "n" puff process in a bottomwater-drive reservoir, *J. Pet. Technol.* **40**, 7, 887–893.

52 Silva L.C.R., Anand M. (2013) Probing for the influence of atmospheric CO_2 and climate change on forest ecosystems across biomes, *Glob. Ecol. Biogeogr.* **22**, 1, 83–92.

53 Chang J., Ciais P., Viovy N., Vuichard N., Herrero M., Havlik P., Soussana J. (2016) Effect of climate change, CO_2 trends, nitrogen addition, and land-cover and management intensity changes on the carbon balance of European grasslands, *Glob. Chang. Biol.* **22**, 1, 338–350.

54 Todd M.R., Grand G.V. (1993) Enhanced oil recovery using carbon dioxide, *Energy Convers. Manage.* **34**, 9–11, 1157–1164.

55 Ahmadbaygi A., Bayati B., Mansouri M., Rezaei H., Riazi M. (2020) Chemical study of asphaltene inhibitors effects on asphaltene precipitation of an Iranian oil field, *Oil Gas Sci. Technol. - Rev. IFP Energies nouvelles* **75**, 6.

56 Ruth D., Wong S. (1990) Centrifuge capillary pressure curves, *J. Can. Pet. Technol.* **29**, 3, 67–72.

57 Barberis Canonica L., Galbariggi G., Bertero L., Carniani C. (1995) Experimental study on asphaltene adsorption onto formation rock: An approach to asphaltene formation damage prevention, *SPE Prod. Facil.* **11**, 3, 156–160.

58 Yan J., Plancher H., Morrow N.R. (1997) Wettability changes induced by adsorption of asphaltenes, *SPE Prod. Facil.* **12**, 4, 259–266.